Hindawi
Geofluids
Volume 2022, Article ID 1796300, 12 pages
https://doi.org/10.1155/2022/1796300

Research Article

Evaluating Gas-Oil Ratio Behavior of Unconventional Wells in the Uinta Basin

Yajie Zhao,[1] Jack Nohavitza,[2] Ryan Williams,[2] Wei Yu,[1,3] Chuxi Liu,[1] Reza Ganjdanesh,[1] and Kamy Sepehrnoori[1]

[1]*Hildebrand Department of Petroleum and Geosystems Engineering, The University of Texas at Austin, Austin, TX 78712, USA*
[2]*EP Energy, Houston, TX 77002, USA*
[3]*Sim Tech LLC, Houston, TX 77494, USA*

Correspondence should be addressed to Wei Yu; yuwei127@gmail.com

Received 7 January 2022; Revised 21 March 2022; Accepted 26 April 2022; Published 11 May 2022

Academic Editor: Andrea Brogi

On account of low matrix permeability and porosity, the fluid phase behavior in tight oil reservoirs significantly differs from the conventional plays, which increases the challenges of evaluating the well performance and providing reliable production prediction. One of the most important efforts is to investigate the behavior of unconventional well gas-to-oil ratio (GOR). The growth trend of GOR is always considered as a principal reference to modify the production strategies and enhance the well productivity. In this paper, long-term GOR (20 years) behavior of an unconventional well model was evaluated by a set of comprehensive sensitivity studies. This model's dimensions and reservoir properties are based on information of the Altamont-Bluebell field in the Uinta Basin. The simulation results established a general framework for interpreting the GOR behavior. Key drivers such as completion designs, reservoir, and fracture properties are investigated. This study provides some key insights into the GOR behaviors, such as the high sensitivity of the hydraulic fracture properties, including fracture conductivity and effective fracture half-length. The GOR behavior could be considerably different on various conductivity values or fracture lengths, resulting from the conductivity impact of phase movement and the pressure transition along the fracture. The fracture design factors like drawdown scenario and cluster spacing also play indispensable roles in impacting the GOR response, where a less aggressive drawdown rate can help to delay the GOR increase at an early stage; a widening spacing also can mitigate the rise of GOR and keep it at low value during the whole production period. The impact from natural fractures is also examined and discussed for the first time, including the effect of natural fracture numbers and conductivity, where the latter variable is considered as a more effective contributor to the GOR prediction. The findings presented in this work promote a better understanding of the GOR behaviors in tight oil reservoirs. Results and discussion in this paper allow a more accurate forecasting production to improve the reservoir management efficiency and provide multiple valuable insights to guide the field development in future projects.

1. Introduction

In view of the growing demand for hydrocarbons from unconventional plays, increased consideration has been given in modifying the production forecasts with more reliable approaches. It is well-known that the subsurface fluid properties and multifluid phase significantly impact the well performance, especially for the solution gas production in tight/shale formations. Therefore, the gas-to-oil ratio (GOR) profile has become one of the essential measures to evaluate production conditions. More attention has been given to unconventional GOR characterization to help to predict long-term gas production trends and modify operation strategies.

Unlike conventional reservoirs with higher permeability, the GOR behavior for shale shows a distinguished paradigm. Whitson and Sunjerga [1] presented a numerical study finding that the producing GOR for unconventional wells is impacted by the flowing bottomhole pressure and the degree of undersaturation, which is different from the conventional

GOR profile that the average reservoir pressure is the main driven factor. Yu [2] emphasized the importance of the solution gas production in tight formations, which intensely affect the GOR increasing speed and longevity due to the gas release. Jones et al. [3] proposed a framework for interpreting idealized GOR behavior in tight black-oil reservoirs; four main GOR stages for unconventional wells were presented in detail: (1) constant GOR at the initial solution GOR (R_{si}); (2) rising GOR as bottomhole flowing pressure (P_{wf}) below the bubble point; (3) GOR plateau; and (4) GOR changes during boundary-dominated flow.

Meanwhile, over the past decade, numerous authors conducted the GOR case studies for unconventional wells from various basins in North America ([4–6], Liu, [7]). Chaudhary et al. [8] provided a numerical study of GOR sensitivities for the unconventional Eagle Ford formation, discussed how the various completion parameters impact GOR, and then emphasized the high sensitivity of the critical gas saturation on oil recovery. Khoshghadam et al. [9] investigated the nanopore proximity effects observed in the Bakken reservoir. The authors discussed how this phenomenon could impact the producing GOR due to bubble-point pressure suppression, critical gas saturation enhancement, and permeability reduction. Jones et al. [3] mentioned a GOR case study in the Woodford formation, where the GOR curve showed a continuous increase without a flattened plateau. The network-type fractures in the Woodford source rock resulted in low conductivity and caused a gradual rise trend of the GOR curve. Dutta et al. [10] studied the GOR trends in the Delaware Basin, where the GOR increased from the west to east along the basin. This study concluded the connection between the GOR behavior and geothermal gradient, TOC, and maturity. Liu et al. [7] also delivered a numerical analysis on the Bakken unconventional GOR by evaluating the difference between historic sliding sleeve and modern plug and perf completion wells.

However, in practice, fracture geometries and reservoir conditions can be highly inconsistent due to the complexity and uniqueness of each unconventional play, which has led to a significant variation in GOR patterns. Despite this, the published GOR studies for each reservoir are still limited; more field case studies on unconventional GOR are required to provide deep insights into GOR behaviors. In addition, for shale/tight oil reservoirs, natural fractures also significantly contribute to the well performance. However, most traditional modeling approaches do not consider the existence of natural fracture networks in their models, which could potentially cause variation in the GOR behaviors. Thus, more in-depth discussions on the impact of natural fractures are also expected.

In this study, a multifractured horizontal well model was constructed to evaluate the unconventional well GOR behavior. The hydrocarbons in the reservoir were characterized according to Altamont-Bluebell volatile oil area. The related reservoir properties were also consistent with validated real subsurface data. Meanwhile, a powerful three-dimensional embedded discrete fracture model (EDFM) was introduced to handle complex fracture geometries in the subsurface. By using the EDFM method, natural fractures can be embedded in regular matrix grids through non-neighboring connections (NNCs), which avoid the gridding issues while keeping the model efficiency and accuracy [11, 12]. The impact of natural fractures on GOR behavior can be analyzed thoroughly and fully comprehended. This study aimed to identify the key impact factors of GOR behavior. Therefore, a number of key parameters were analyzed orderly and discussed rigorously. Furthermore, the impact of natural fractures on the GOR trend involving the fracture conductivity and fracture number was also investigated. This study is the first attempt to demonstrate GOR characterization using the EDFM method with consideration of natural fractures. The learnings shown in this paper can help to modify production strategy and improve production forecasting for future projects.

2. General Geology

The interest area of this study focuses on the Uinta Basin, as shown in Figure 1, which is made up of naturally fractured, tight oil sands with multiple pay zones. The Uinta Basin is an asymmetric east-west trending basin with a steep flank bounded at the north and a gently sloping flank. The Altamont-Bluebell field, one of the largest developing oil fields in North America, is located in the Duchesne and Uintah counties, along with the north-central portion of the Unita Basin [13]. Production of oil, gas, and associated hydrocarbons is mainly from the upper Green River, lower Green River, and Green River/Wasatch formations. The tight oil reservoir of the lower Green River is the focus area of this study.

The lower Green River formation is made up of highly fractured sandstones, shales, siltstones, and dolomites [15]. The producing interval of the Lower Green River and Wasatch formations ranges from 9,500 ft. to 16,500 ft, which is deeper and thinner at the northeast of the Bluebell field and thickens towards the extreme southwest portion of the Altamont-Bluebell field. In this formation, natural fracture networks are well developed and also impact the flow capacity [16]. The average bottomhole temperature of this producing interval is around 240°F, and the reservoir pressure ranges from 7,000 psi to 9,000 psi.

3. Modeling Natural Fractures with EDFM

EDFM is an efficient solution to model complex fracture geometries in numerical simulation. It has been implemented successfully in various studies and proved its flexible and reliable performance [17–20]. In this method, fractures are embedded into the matrix grids by discretizing each fracture plane into smaller segments based on the matrix-cell boundaries [12, 21]. This approach avoids the gridding issues of the traditional LGR approach and also improves the model efficiency compared to the unstructured gridding technique [19, 22]. By applying EDFM, nonneighboring connections (NNCs) are introduced to mimic the flow communication between the segments that are connected physically but not neighboring in the computational domain [11].

Generally, EDFM considers four types of connections between well, fracture, and matrix. Except for the basic

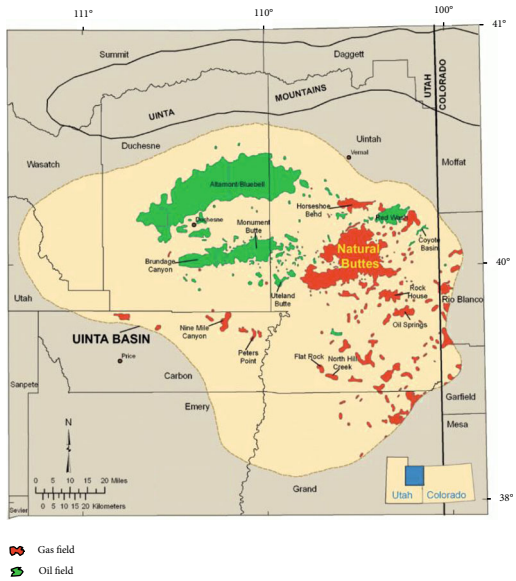

Figure 1: Map showing the study area of the Altamont-Bluebell field in Uinta Basin [14].

connection between matrix grids, EDFM also introduces three types of NNCs to represent the fluid flow associating with the fracture segments, as presented in Figure 2. The NNCs consider the flow between fracture segments within a single fracture, the flow between intersecting fracture segments within different fractures, and the flow between matrix grid blocks and the corresponding fracture segments. The following equation describes the NNC transmissibility factor (T_{NNC}) for the last three kinds of connections [11]:

$$T_{\mathrm{NNC}} = \frac{k_{\mathrm{NNC}} A_{\mathrm{NNC}}}{d_{\mathrm{NNC}}}, \tag{1}$$

where k_{NNC} is the permeability associated with the connection, A_{NNC} is the contact area between the NNC pair, and d_{NNC} corresponds to the distance between the NNC pair.

In addition, the flow between fractures and wells is also considered in the EDFM, which is presented as the perforation dots in both well and fracture segments, as shown in Figure 2(b). An effective well index (WI) for the well-fracture connection is employed by the modified Peaceman equation as follows:

$$\mathrm{WI} = \frac{2\pi k_f w_f}{\ln\left(r_e/r_{\mathrm{w}}\right)}, \tag{2}$$

$$r_e = 0.14\sqrt{L^2 + W^2}, \tag{3}$$

where k_f is the fracture permeability, w_f is the fracture aperture, r_e is the effective radius, r_w is the wellbore radius, L is length of the fracture segment, and W corresponds to height of the fracture segment.

4. Model Overview

4.1. Model Constructions. In this study, a multistage horizontal well is built to investigate the effect of reservoir properties, fracture characteristics, and the completion designs on GOR prediction. The subject well is set at 10163 ft vertical depth with 9880 ft lateral length. There are 131 hydraulic fractures with average fracture spacing of 75 ft. The effective fracture length is assumed to be 150 ft with a fracture conductivity of 100 md-ft. The associated reservoir model is presented in Figure 3.

The relative permeability parameters used for the GOR characterization are shown in Figure 4. Meanwhile, in order to better describe the reservoir fluid properties, the model is assigned to be a volatile oil type, which is mainly dominated by the group C_7-C_{10} and C_{11}-C_{20} (Figure 5). Furthermore, Table 1 lists the reservoir properties that were utilized in this simulation study. All these reservoir properties in the numerical model are based on real subsurface data from the Altamont-Bluebell field in the Uinta Basin and then be validated and calibrated through history matching with the available production records from the wells at the same production area.

4.2. GOR Behavior Analysis for the Base Model. Figure 6 displays the base case simulation results for bottomhole flowing pressure and instantaneous GOR versus time. The GOR curve can be divided into four stages, which are considered as typical GOR behavior for unconventional wells, as mentioned previously [3]. It is clear to observe that at the beginning of the production, GOR remains constant as long as the bottomhole flowing pressure is higher than the bubble point. During this period, only oil is flowing without increasing in gas saturation. After the bottomhole pressure drops less than the bubble point, the pressure gradient starts changing, which results in a remarkable rise in gas saturation; thereby, the GOR starts to rise. The rising trend could be stopped when the bottomhole flowing pressure reaches the minimum and stay constant. A "plateau" might occur and constrains the gas movement, where the gas saturation is stabilized during the stage of transient linearly flow at a constant bottomhole pressure. In this base model, the GOR plateau can be clearly detected and last for two to three years. At the middle to late time of production (labeled as stage 4), the drainage area keeps expanding, leading to the beginning of boundary-dominated flow (BDF). During this period, the gas saturation develops at the fracture surface, and GOR turns to rise again. It is noted that the existence of each stage, the length scale of the stage period, and even the shape and the rate of GOR rise are determined by multiple complicated factors from subsurface and operation, which also explained the necessity of providing more GOR characterization study because of its high complexity and sensitivity.

5. Sensitivity Analysis of GOR Behavior

As mentioned in the previous section, GOR trends could be highly influenced or even controlled by diverse subsurface conditions or operation scenarios. The objective of this study is to investigate the possible influential factors with their

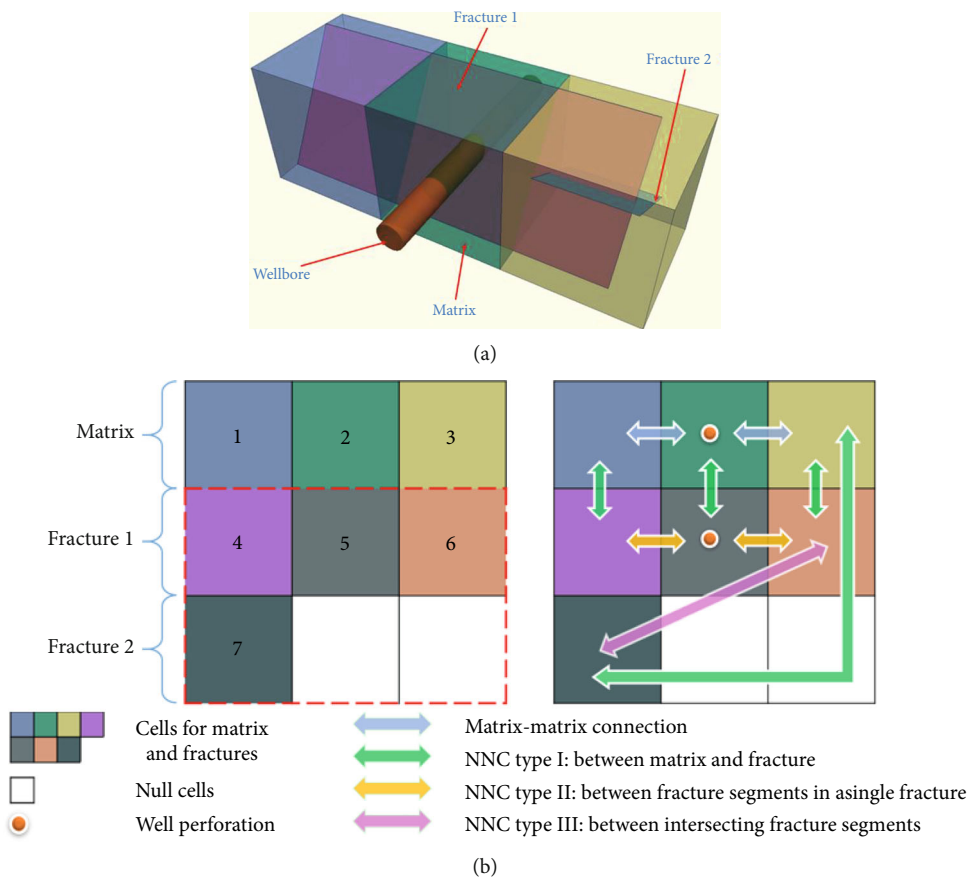

Figure 2: Explanation of embedded discrete fracture model (EDFM): (a) a physical domain with three matrix blocks, two fractures, and a wellbore, and (b) a computational domain shows the connections within each discretized cell. The arrows show the different types of nonneighboring connections (NNCs) [11].

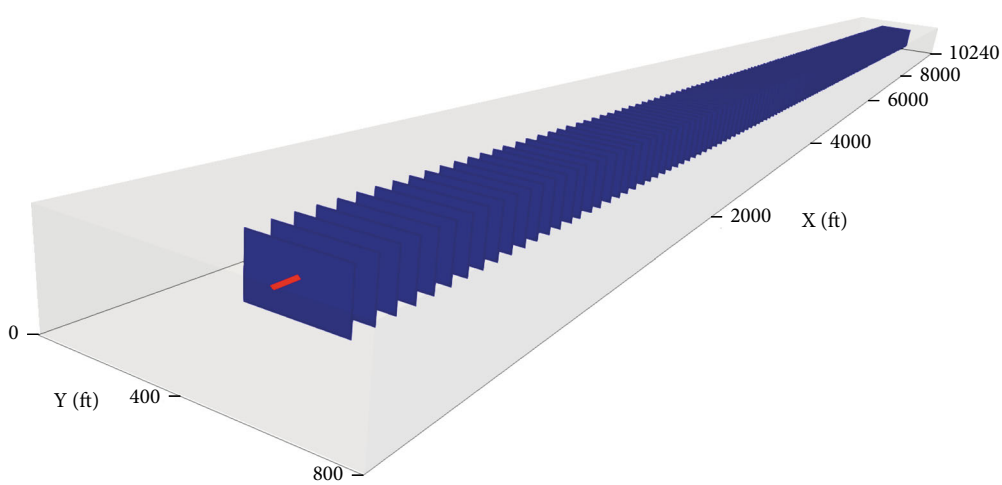

Figure 3: A tight oil reservoir model including a horizontal well with multistage hydraulic fractures. The red line represents wellbore, and the blue rectangle represents hydraulic fractures.

impact on GOR prediction and then to find out the logical explanation behind different performances. Therefore, on the basis of the GOR stages identified in the base model, we examined multiple GOR trend drivers from various aspects and provided in-depth discussions.

5.1. Impact of Reservoir Permeability. Reservoir permeability is a determinant factor for evaluating the well productivity. Compared to the base model with 0.001 millidarcies shown as the red curve in Figure 7, a notable difference can be seen from the other two GOR curves with lower matrix

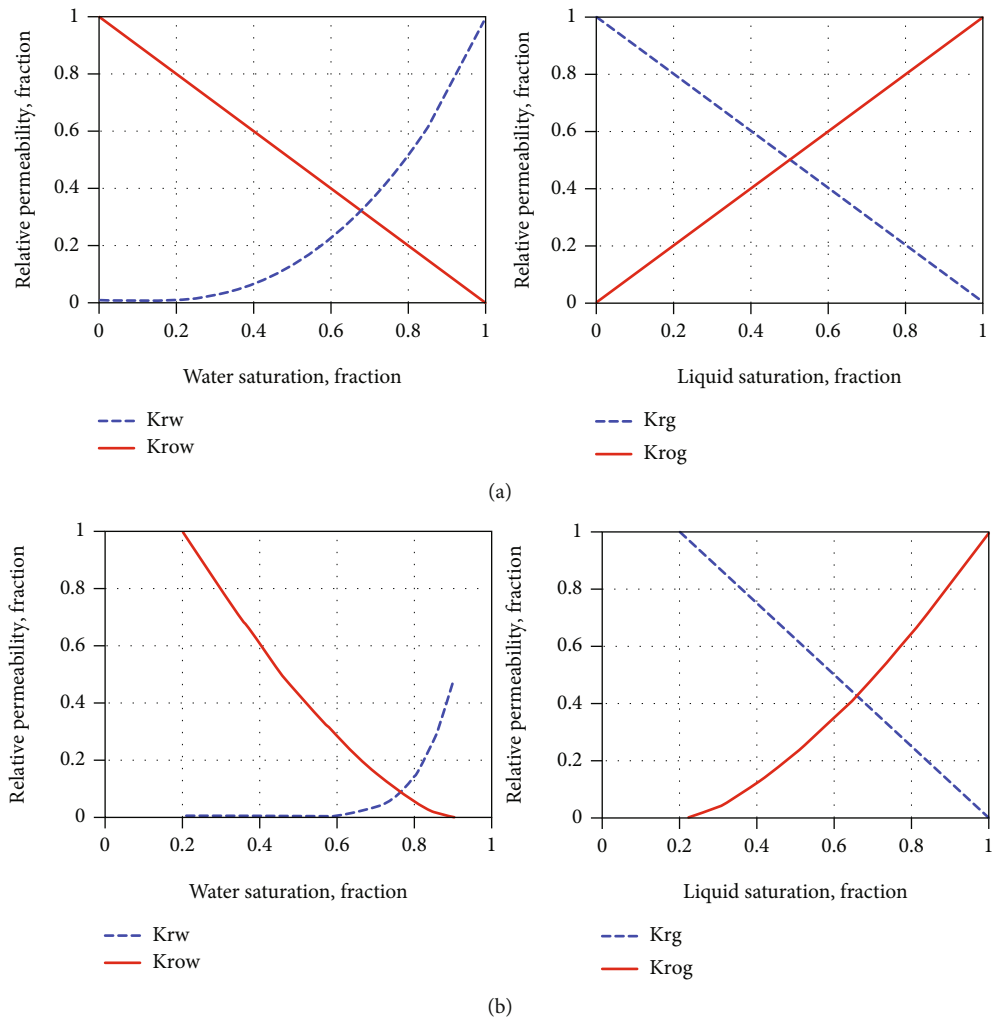

Figure 4: Three-phase relative permeability curves of: (a) fractures and (b) matrix in this study for modeling unconventional oil reservoirs.

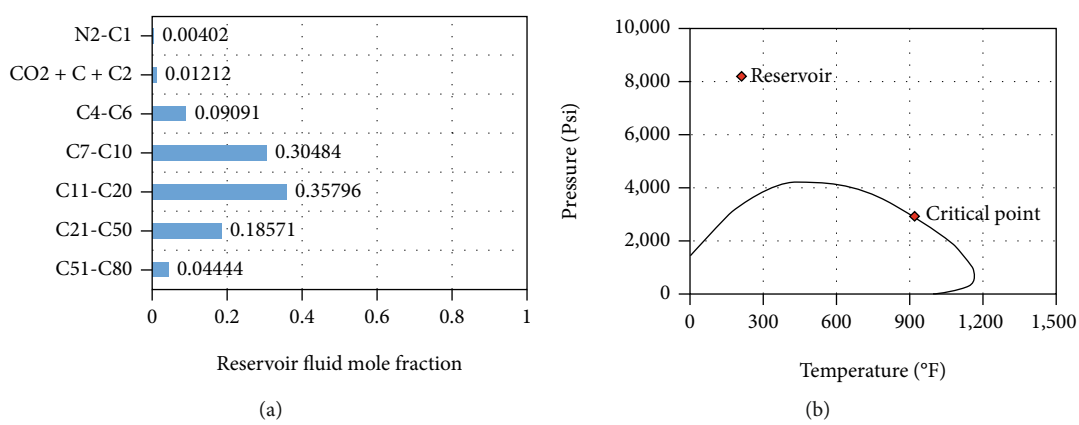

Figure 5: Reservoir fluid properties of: (a) composition and (b) P-T diagram with marked initial reservoir condition and critical point.

permeability (horizontal). It is acknowledged that higher reservoir permeability can provide stronger support for production, especially when the matrix starts draining into the fracture networks. When it continues, the oil production from the matrix will contribute more and, relatively, result in a faster decrease in gas production rate. Therefore, reservoir with higher permeability always shows a slow-growing trend of the producing GOR.

Table 1: Basic reservoir properties used in the field-scale shale-gas models.

Reservoir description	Value	Unit
Model dimension ($x \times y \times z$)	$10240 \times 800 \times 275$	Ft
Number of grid blocks ($x \times y \times z$)	$256 \times 20 \times 9$	—
Grid blocks dimensions ($x \times y \times z$)	$40 \times 40 \times 25$	Ft
Reservoir depth (top)	10025	Ft
Initial reservoir pressure	8200	Psi
Bubble point pressure	4330	Psi
Reservoir temperature	210	°F
Matrix water saturation	0.47	—
Matrix permeability	0.001	md
Matrix porosity	0.09	—

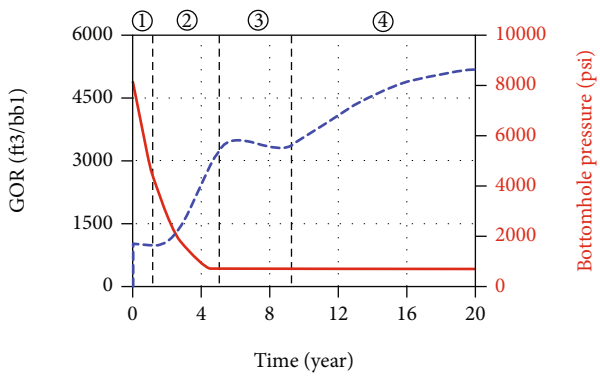

Figure 6: Simulation results of the base model GOR behavior. Four stages can be clearly observed, consistent with the pressure drawdown profile.

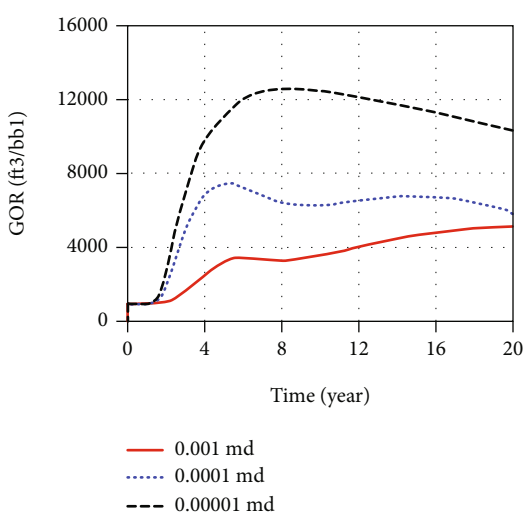

Figure 7: Simulated cases showing dependence of GOR on matrix permeability (horizontal). Higher matrix permeability gives stronger support and help to mitigate the GOR rise.

When it comes to unconventional reservoir study, the anisotropy in permeability also needs to be taken into account. In the numerical simulation, it is always set as a multiplier value to represent the ratio of vertical to horizontal permeability. Figure 8 displays the GOR trends under three various vertical permeability multipliers. At the early stage of production, higher vertical permeability gives more robust matrix support and lowers the GOR rise, consistent with the previously described. However, the trends start to change in the mid- to late-term production because of the gravity impact. When the gas saturation exceeds the critical gas saturation, the gas begins to flow to the wellbore. At the same time, the gas in the reservoir also moves vertically due to gravitational forces. A larger multiplier value, which implies a higher vertical permeability, will lead to more gas produced through vertical movement and thus increase the GOR gradually.

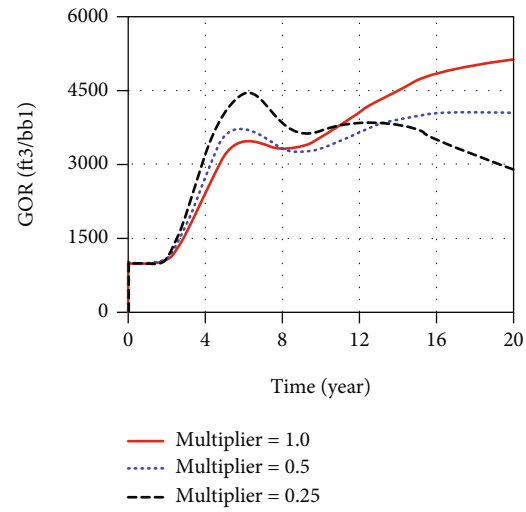

Figure 8: Simulated cases showing dependence of GOR on matrix multiplier (the ratio of vertical to horizontal permeability). Larger multipliers enhance the gas movement and then increase the GOR rise in the late time production.

5.2. Impact of Completion Design. In addition to the impact of reservoir properties, the design of completion and operation strategies also shows a critical importance on the trend of well GOR. In this section, two of the biggest drivers are selected and evaluated in depth: the pressure drawdown strategy of the well and the designed cluster spacing of the hydraulic fractures.

5.2.1. Effect of Drawdown Strategy. Figure 9 shows the GOR prediction of three sequential drawdown scenarios in order which were labeled as conservative, moderate, and aggressive strategies. It can be seen that when the bottomhole pressure falls below the bubble point, a more aggressive drawdown leads to a quicker GOR rise, while the conservative drawdown delays the GOR rise significantly. However, the conservative drawdown also gives a higher peak of the GOR. The influence of these three cases is also negligible at the late time of production. One of the potential explanations is that a conservative strategy can keep bottomhole pressure above the bubble point at the early stage of production for a longer time. This type of strategy constrains the amount of fluid

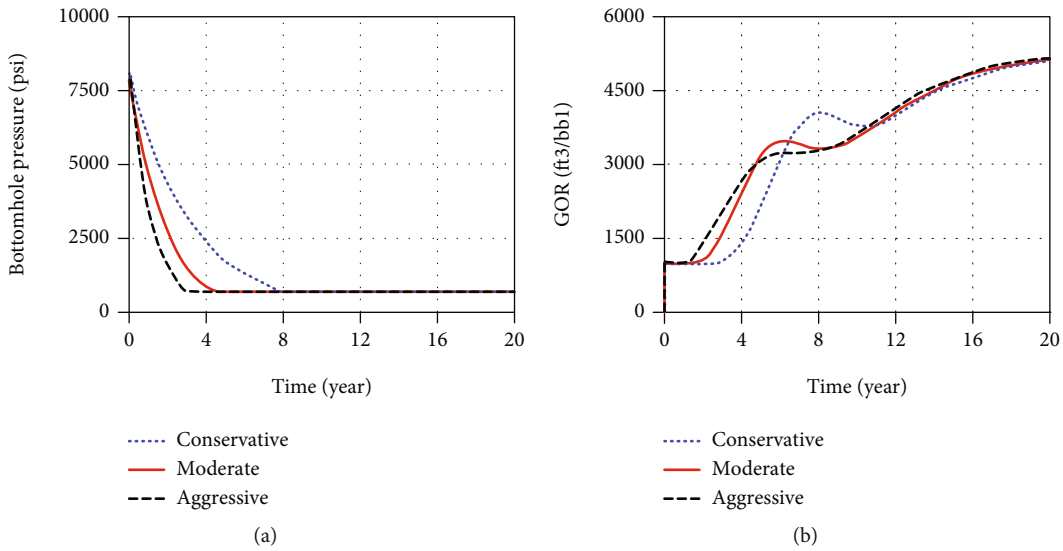

Figure 9: Simulated cases showing dependence of GOR on pressure drawdown strategy: (a) three drawdown scenarios from conservative strategy to aggressive strategy and (b) GOR responses under different pressure drawdowns.

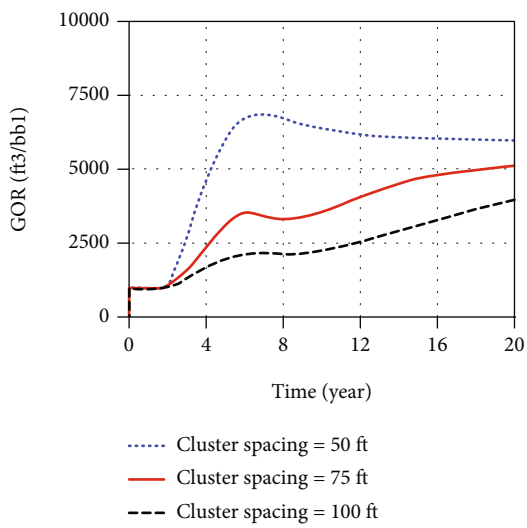

Figure 10: Simulated GOR vs. time for various fracture spacings (50-100 ft). Widening cluster spacing can effectively mitigate the GOR increasing rate.

produced so that the back pressure on the formation can keep stable at a higher wf. Therefore, the GOR would not rise as quickly as the aggressive drawdown due to the delay effect from the formation. Nevertheless, when the pressure reaches the minimum and keeps at constant, the drawdown scenario no longer affects the change of GOR curves. For long-term production, the GOR trends gradually become similar if all other completion design parameters are kept the same. It is also a good example to show the importance of performing long-term production forecasts to allow a more comprehensive understanding of well performance and associated GOR prediction.

5.2.2. Effect of Cluster Spacing. As shown in Figure 10, the determination of the cluster spacing is extremely important to influence GOR. For all scenarios, GOR starts rising at the same time. However, wells with more close-spaced fractures show a steeper GOR rise with time. This is because wider spacing could create a larger drainage area per fracture, which will help to delay the production interference between fractures. Hence, the well productivity can be enhanced with a lower GOR curve.

5.3. Impact of Fracture Properties. As is well-known that hydraulic fracturing is the most critical implementation in unconventional reservoir development, the effectiveness of fracturing will directly determine the success of well productivity. In this section, two principal sensitivities, fracture conductivity and effective fracture half-length, are brought to discussion separately to evaluate their influences on the GOR performance.

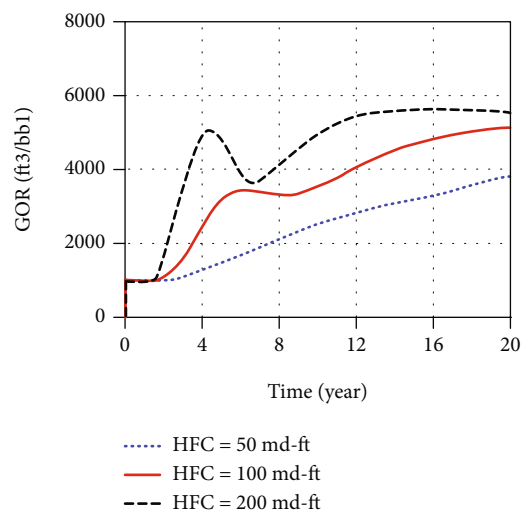

Figure 11: Effect of hydraulic fracture conductivity on GOR rise versus time. Fractures with high conductivity lead to a steep GOR rise rate.

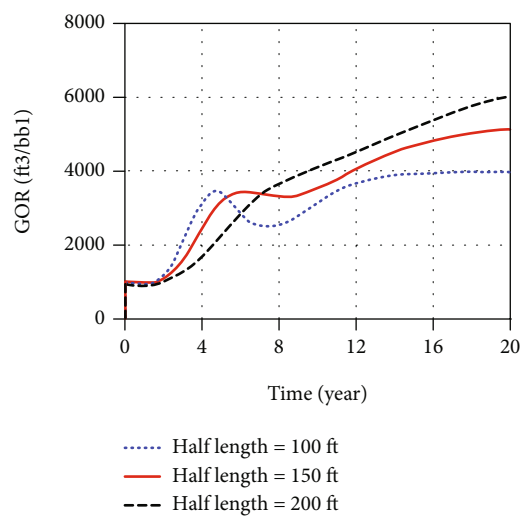

Figure 12: Effect of hydraulic fracture half-length on GOR rise versus time. Fractures with longer length leads to a mitigation in GOR rise.

5.3.1. Effect of Hydraulic Fracture Conductivity. The first simulation result to present is the GOR behavior based on three cases with different fracture conductivities: 50 md-ft, 100 md-ft, and 200 md-ft, as shown in Figure 11. The first observation is the mitigation effect of GOR rise as the conductivity becomes lower. This is because for fractures with finite conductivity, the pressure in fractures is not uniformly distributed. It will increase away from the wellbore from P_{wf}. Therefore, fractures with lower conductivity can slow the pressure transition and then relieve the rising rate of GOR.

The second key observation is that lower fracture conductivity helps to mitigate the GOR "hump." This hump is commonly seen in the simulation with high conductivity fractures, especially when the P_{wf} reaches to the minimum value; the GOR curve might show a "hump" before it goes to the transient GOR plateaus. In some cases, it can last for a long time, so that in stage three, the GOR plateau will be easily overlooked or even no longer exist. One explanation for this phenomenon is that when the P_{wf} stops decreasing, as a response to the pressure recovery, some of the gas will be restricted by the sudden change of pressure gradient and "held" in the fractures, resulting in the decline of gas production.

5.3.2. Effect of Fracture Half-Length. Figure 12 reveals the effect of effective fracture half-length on the GOR behavior. Similar to the reason discussed in fracture conductivity, for finite conductivity fractures, longer fracture has a greater delaying effect due to the time cost of pressure transition. However, the trend inversed at the late term of production, which could be explained by the enlarged drainage area caused by the longer fracture. Meanwhile, it is also worth noting that the well with longer fracture length has no plateau occurrence. This is because the time of initial GOR rise lasts so long as it continues into boundary-dominated flow obscuring the plateau, as discussed previously.

5.4. Impact of Natural Fractures. Natural fractures are always distributed heterogeneously in the reservoir. In this reservoir

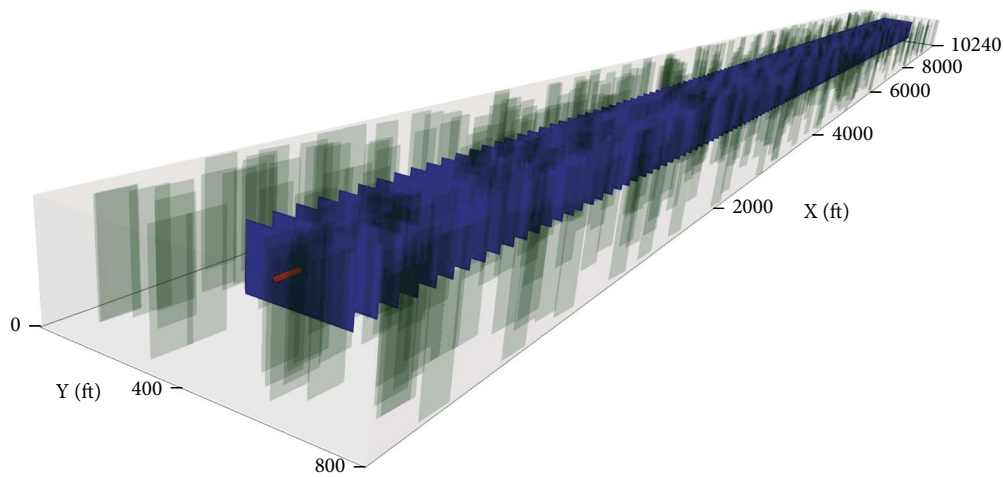

Figure 13: 800 natural fractures are embedded into the base model. The green rectangle represents vertical natural fracture.

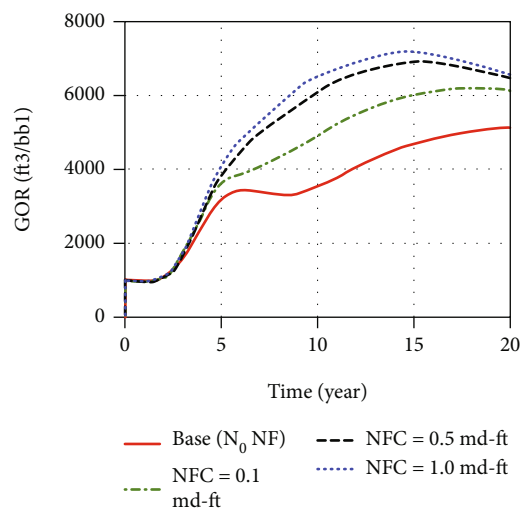

Figure 14: Comparison of 20-year GOR prediction with different natural fracture conductivity (NFC) ranges from 0.1 to 1.0 md-ft.

model, as shown in Figure 13, one set of natural fractures is embedded into the formation, with a striking angle that is perpendicular to the wellbore direction. All these natural fractures are generated randomly in the whole reservoir area. The length of the natural fractures is assigned at 100 ft, while the fracture height is fixed and assumed to be the same as the reservoir thickness. The dip angles of all natural fractures are assumed to be 90 degrees or vertical. In this section, sensitivity studies on the influence of natural fracture are conducted by the EDFM approach. Case studies on the influence of natural fracture conductivity and numbers are conducted.

5.4.1. Effect of the Natural Fracture Conductivity (NFC). The impact of natural fracture conductivity on well GOR was the first factor to be investigated. For the three cases with 800 natural vertical fractures, the conductivities of fractures are assigned at 0.1 md-ft, 0.5 md-ft, and 1.0 md-ft, respectively. Figure 14 shows the comparison results of the GOR prediction among these scenarios. The base case without natural fractures is also included in the plot. The result shows that the GOR trend is highly susceptible to the natural fracture conductivity for a long production term. As natural fractures contribute to the production, the GOR trend also increases, indicating a more active gas movement from the reservoir to the wellbore. In addition, when the fracture conductivity keeps increasing, the natural fractures will approach the infinite conductivity. The relative contribution from natural fractures thus does not change notably. Therefore, the difference between the GOR trends gradually decreases.

5.4.2. Effect of the Number of Natural Fractures. There is no doubt that natural fractures could play a vital role in well performance. As more natural fractures exist, the conductivity and connectivity between reservoir and well will be stronger. Hence, the well productivity can be enhanced. In this section, four sets of natural fractures with different numbers (200, 400, 800, and 1600) are generated by using the EDFM method. Meanwhile, each combination is simulated with

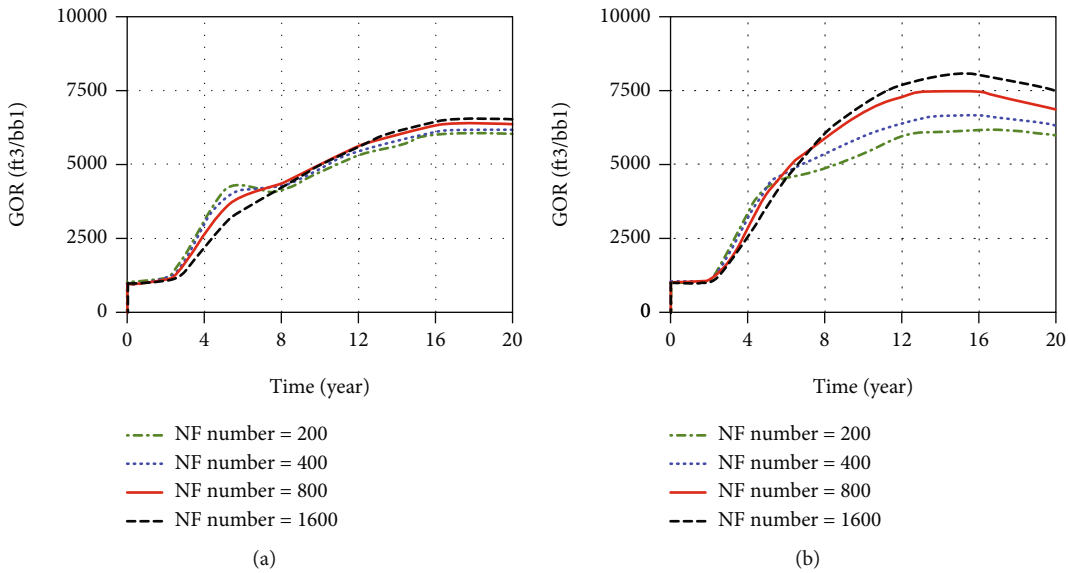

Figure 15: Comparison of 20-year GOR prediction with different numbers of natural fractures under 2 different settings of natural fracture conductivity (NFC): (a) low conductivity at 0.1 md-ft and (b) high conductivity at 1 md-ft.

both low and high natural fracture conductivity. The simulation results for the well GOR are presented in Figure 15. When the number of natural fractures increases, more natural fractures will start participating in the production, and the gas phase will be easier to move under the pressure decay. However, more natural fractures also mean more time consuming for the pressure transition, which could explain the steeper rise of the case with less natural fractures at the very early stage. As the production process continues, more gas could move through the passes between the hydraulic fractures and natural fractures and then be produced from the wellbore. Therefore, the GOR curve keeps rising and maintains a high value. However, this type of difference is strongly dependent on the conductivity of natural fractures, which can be clearly investigated from the comparison between Figure 12(a) and Figure 12(b). For natural fractures with lower conductivity, the contribution becomes weaker, which leads to fewer differences between the GOR behaviors. It can be concluded that conductivity is still the primary factor for the natural fractures to influence productivity and GOR behaviors.

6. Conclusions

This study demonstrates an unconventional well model in the Uinta Basin to conduct GOR sensitivity analysis by applying the nonintrusive EDFM method along with a third-party reservoir simulator. In this paper, a comprehensive analysis and in-depth discussion of GOR behavior are presented. The main conclusions can be drawn as follows:

(1) The unconventional reservoir GOR behavior is highly sensitive to reservoir permeability. In general, higher permeability helps to enhance the supporting effect from the matrix and maintain the GOR at a lower rate. Meanwhile, the anisotropy on the vertical direction also needs to be considered as a principal factor for the GOR prediction. The gas movement due to gravitational force could change the GOR trend notably, especially for long-term production

(2) The sensitivity study also illustrates several key drivers from operation strategy and hydraulic fracture properties, including drawdown strategy, fracture/cluster spacing, fracture conductivity, and fracture half-length. All parameters are simulated under 20 years of production. The long-term prediction clearly shows the GOR behavior changes from short to long, which effectively improved understanding of the control factors for GOR behaviors under different stages

(3) This study is the first time analyzing the impact of natural fractures on GOR behavior by using EDFM, which is a practical approach for simulating the flow behavior under complex fracture networks. The number of fractures directly influences the conductivity and connectivity between the reservoir and well. Higher numbers show higher GOR trends for long-term production. However, natural fracture conductivity can severely affect the GOR difference between GOR numbers, which is a key parameter to impact the oil/gas phase movement from the reservoir to the stimulated area. From the result in this study, NFC is considered as the main controller impacting natural fractures' contribution on GOR prediction

Nomenclature

EDFM: Embedded discrete fracture model
LGR: Local grid refinement
NNCs: Nonneighbor connections

T_{NNC}: NNC transmissibility factor
k_{NNC}: Permeability associated with the connection
A_{NNC}: Contact area between the NNC pair
d_{NNC}: Distance between the NNC pair
w_f: Fracture width or fracture aperture
k_f: Fracture permeability
r_e: Effective radius
r_w: Wellbore radius
L: Fracture segment length
W: Fracture segment height
GOR: Gas-to-oil ratio
P_{wf}: Bottomhole flowing pressure
R_{si}: Initial solution GOR
NFC: Natural fracture conductivity.

SI Metric Conversion Factors

ft × 3.048 e-01: m
ft^3 × 2.832 e-02: m^3
cp × 1.0 e-03: Pa·s
psi × 6.895 e+00: kPa
md × 1e-15 e+00: m^2

Data Availability

All data used to support the findings of this study are available from the corresponding author upon request.

Conflicts of Interest

The authors declare that they have no conflicts of interest.

Acknowledgments

The authors would like to acknowledge technical and data support from Sim Tech LLC for providing the EDFM software for this study.

References

[1] C. H. Whitson and S. Sunjerga, "PVT in liquid-rich shale reservoirs," in *Paper SPE 155499, Presented at the SPE Annual Technical Conference and Exhibition*, pp. 8–10, San Antonio, Texas, 2012.

[2] S. Yu, "A new methodology to forecast solution gas production in tight oil reservoirs," in *Paper SPE 171580, Presented at the SPE/CSUR Unconventional Resources Conference*, Canada, Calgary, Alberta, 2014.

[3] R. S. Jones, "Producing-gas/oil-ratio behavior of multifractured horizontal wells in tight oil reservoirs," *SPE Reservoir Evaluation & Engineering*, vol. 20, no. 3, pp. 589–601, 2017.

[4] M. L. Carlsen, C. H. Whitson, A. Alavian et al., "Fluid sampling in tight unconventionals," in *Paper SPE 196056, presented at the SPE Annual Technical Conference and Exhibition*, Calgary, Alberta, Canada, 2019.

[5] F. Male, A. Gherabati, J. Browning, M. Marder, and S. Ikonnikova, "Forecasting production from Bakken and three forks wells using a segregated flow model," in *Paper URTeC 2666809, presented at the SPE/AAPG/SEG Unconventional Resources Technology Conference*, pp. 24–26, Austin, Texas, 2017.

[6] Y. Pradhan, "Observed gas-oil ratio trends in liquids rich shale reservoirs," in *Paper URTeC 3229, presented at the SPE/AAPG/SEG unconventional resources technology conference, virtual*, pp. 20–22, 2020.

[7] Y. Liu, B. Coffman, N. McMahan, and F. Alisdair, "Bakken unconventional well gas-oil ratio (GOR) behavior characterization," in *Paper URTeC 5358, presented at the SPE/AAPG/SEG unconventional resources technology conference*, pp. 26–28, Houston, Texas, 2021.

[8] A. S. Chaudhary, C. A. Ehlig-Economides, and R. A. Wattenbarger, "Shale oil production performance from a stimulated reservoir volume," in *Paper SPE 147596, presented at the SPE annual technical conference and exhibition*, Denver, 2011.

[9] M. Khoshghadam, A. Khanal, and W. J. Lee, "Numerical study of impact of nano-pores on gas-oil ratio and production mechanisms in liquid-rich shale oil reservoirs," in *Paper URTeC 2154191, Presented at the SPE/AAPG/SEG Unconventional Resources Technology Conference*, pp. 20–22, San Antonio, Texas, USA, 2015.

[10] R. Dutta, S. Dawson, and M. Michael, "Is GOR truly affecting recovery? A multi-variate case study in the Delaware Basin," in *Paper URTeC 2903134, presented at the SPE/AAPG/SEG unconventional resources technology conference*, pp. 23–25, Houston, Texas, 2018.

[11] Y. Xu, J. S. A. Cavalcante Filho, W. Yu, and K. Sepehrnoori, "Discrete-fracture modeling of complex hydraulic-fracture geometries in reservoir simulators," *SPE Reservoir Evaluation & Engineering*, vol. 20, no. 2, pp. 403–422, 2017.

[12] W. Yu and K. Sepehrnoori, *Shale Gas and Tight Oil Reservoir Simulation*, Elsevier, Cambridge, USA, 1st edition, 2018, ISBN: 978-0128138687.

[13] H. B. Lynn, R. Bates, M. Layman, and M. Jones, "Natural fracture characterization using P-wave reflection seismic data, VSP, borehole imaging logs, and the in-situ stress field determination," in *Paper SPE 29595, Presented at the Low Permeability Reservoirs Symposium*, pp. 19–22, Denver, Colorado, 1995.

[14] C. T. Chidsey, "Energy news: natural buttes field – Utah's "tight" sandstone gas warehouse," *Survey Notes*, vol. 43-2, p. 8, 2011.

[15] T. D. Fouch, V. F. Nuccio, J. C. Osmond, L. MacMillan, W. B. Cashion, and C. J. Wandrey, "Oil and gas in uppermost cretaceous and tertiary rock, Uinta Basin, Utah," *Utah Association Guidebook*, vol. 20, pp. 9–47, 1992.

[16] W. Narr and J. B. Currie, "Origin of fracture porosity – example from Altamont field," *Utah. AAPG*, vol. 66, no. 9, pp. 1231–1247, 1982.

[17] A. Moinfar, A. Varavei, K. Sepehrnoori, and R. T. Johns, "Development of a novel and computationally-efficient discrete-fracture model to study IOR processes in naturally fractured reservoirs," in *Paper SPE 154246, presented at the SPE Improved Oil Recovery Symposium*, pp. 14–18, Tulsa, Oklahoma, 2012.

[18] M. Shakiba and K. Sepehrnoori, "Using embedded discrete fracture model (EDFM) and microseismic monitoring data to characterize the complex hydraulic fracture networks," in *Paper SPE 175142, presented at the SPE Annual Technical Conference and Exhibition*, pp. 28–30, Houston, Texas, 2015.

[19] Y. Xu, W. Yu, N. Li, E. Lolon, and K. Sepehrnoori, "Modeling well performance in Piceance Basin Niobrara formation using embedded discrete fracture model," in *Paper URTeC 2901327,*

presented at the SPE/AAPG/SEG Unconventional Resources Technology Conference, pp. 23–25, Houston, Texas, 2018.

[20] Y. Xu, W. Yu, and K. Sepehrnoori, "Modeling dynamic behaviors of complex fractures in conventional reservoir simulators," *SPE Reservoir Evaluation & Engineering*, vol. 22, no. 3, pp. 1110–1130, 2019.

[21] Y. Xu and K. Sepehrnoori, "Development of an embedded discrete fracture model for field-scale reservoir simulation with complex corner-point grids," *SPE Journal*, vol. 24, no. 4, pp. 1552–1575, 2019.

[22] W. Yu, Y. Xu, R. Weijermars, K. Wu, and K. Sepehrnoori, "A numerical model for simulating pressure response of well interference and well performance in tight oil reservoirs with complex-fracture geometries using the fast embedded-discrete-fracture-model method," *SPE Reservoir Evaluation & Engineering*, vol. 21, no. 2, pp. 489–502, 2018.